Section A-Research paper

Quantum chemical investigations on a supramolecular porphyrin-fulleropyrrolidine dyads for photovoltaic devices

Shalmali Bhattacharya[(a)], Shiv Sankar Saha[(b)], Subrata Nayak[(b)], Soumya Chatterjee[(c)], Shrabanti Banerjee[(d)], Sumanta Bhattacharya[(b)]*

(a) Department of Computer Science Engineering, Academy of Technology, Adisaptagram, Hooghly, West Bengal -712 502, India.

(b) Department of Chemistry, The University of Burdwan, Golapbag, Burdwan – 713 104, India.

(c) Department of Physics, Academy of Technology, Adisaptagram, Hooghly, West Bengal - 712 502, India.

(d) Department of Chemistry, Raja Rammohan Roy Mahavidyalaya, Radhanagar, Hooghly, West Bengal – 712 406.

Abstract

The present paper deals with the estimation of conformational stability and determination of electronic structures of H_2-porphyrin-fulleropyrrolidine (**1**) and zincporphyrin–fulleropyrrolidine (**2**) dyadsby*ab initio* (HF)and density functional theory (DFT) calculations in *vacuo*. In dyads **1** and **2**, fulleropyrrolidineis directly linked to the tetrapyrrolic rings by ethylene subunits. Both HF and DFTcalculations establish that possibility of photoinduced electron transfer (PET) phenomenon is higher in case of **2** compared to **1**.Investigation on frontier molecularorbitals at different electronic states reveal that the highest occupied molecularorbital and thelowest unoccupied molecular orbital of thesesupramolecules is delocalized due to PET phenomenon. Generation of molecular electrostatic potential (MEP) maps by both HF and DFT calculations substantiate the PET phenomenon (as stated above) and establish that the direction of electron transfer occurs from the porphyrin subunits to the fulleropyrrolidine in dyads **1** and **2**.

Keywords: H_2-(**1**) and zincporphyrin-fulleropyrrolidine (**2**) dyads; HF and DFT calculations; conformational stability; HOMO-LUMO energy gap; MEP.

*author for correspondence; Email: sbhattacharya@chem.buruniv.ac.in

1. Introduction

Over the past few decades, electron transfer (ET) and energy transfer (EnT) phenomena have been intensively studied for biological and artificial molecular systems [1−8]. In recent past, design and construction of photovoltaic devices is considered to be one of the most importantareas of researchasgeneration of photovoltaic elements willcertainly restrict cost effectiveness, produce more efficient, and more environmentally friendly devices [9,10]. In this context, various covalently and non-covalently linked systems have been constructed in order to mimic the photoinduced ET (PET) process [11]. These systems are constructed on the basis of the concept of donor(D)-acceptor(A) pair theory.

For the construction of potential molecular architecture as a result of EDA interactions, both porphyrins [12,13] and fullerenes [14-16] have been extensively utilized as efficient building blocks for their typicalphysicochemical [17] and photophysical properties [18]. The porphyrin-fullerene conjugates are of remarkableutilitydue to their electronic complementary [19-21] and spontaneous interaction between porphyrin and fullerene [22-34]. Due to the presence of conjugated π-system, porphyrin macrocycle can absorb light in the spectral range of wide variety and as a result of this porphyrins may be suitably employedin the preparation of light-harvesting antennas [35]. In contrast, due to forbidden singlet-singlet transitions,fullerenes and functionalized fullerenes exhibit fragile light absorption in the visible and near infrared regions [36]. However, fullerenes are considered to be excellent electron acceptors [37-40]. In view of this consolidation, porphyrin-fullerene molecular assemblies are extensively utilized for the construction of photosynthetic models and to mimic artificial PET processes which efficiently harvest solar energy [41-44]. Therefore, porphyrin-fullereneconjugatesarecontemplated as essential componentsin various photoelectrical devices [45], in the preparation of nanocomposite materials [46] which

actually leads to the advancement of nanotechnology [47]. Apart from this, porphyrin-fullerene conjugates find potential prospect in the fieldsofpharmaceutical and medical sciences [48].

In recent past, porphyrin-fullerene dyad system gainsconsiderable interest due to some characteristic features like interesting optoelectronic properties andtheirapplications in devising organic solar cells [49]. Several molecular donor-acceptor types systems arestudiedanddeveloped including donor-acceptor dyads with more complex and flexible linkers [50]along withdesign of multiple donor-acceptor couple [51]. Very recently, Porku et al. have highlighted the molecular design and chemical versatility of azobenzene dyads containing porphyrin, fullerene C_{60} and pyrene [52]. Sissaoui et al. have nicely demonstrated the PET phenomenon in a porphyrin-fullerene dyad system in which porphyrin analogue gets adsorbed at the dodecane/water interface [53]. Through conjugated bridges, interfacingporphyrin-tetrapyridylC_{60} dimers are prepared which shows remarkable ultrafast charge separation [54].Using the formation of self-assembled monolayers for porphyrin-fullerene dyad system, an advanced version of organic optical memory device has been generated [55]. Very recently, Tkachenko has nicely demonstrated the effect of donor/acceptor size on rate of PET [56].

Therefore, study of conformational stability and electronicstructures of the supramolecular dyad(s) comprising porphyrin and fullerene represents timelyresearchon the context of cited work as mentioned above. The present work highlights thephenomenon of PET mechanism in supramolecular dyads, namely, octaethyl free-base porphyrin-fulleropyrrolidine (**1**)and octaethylzincporphyrin-fulleropyrrolidine (**2**)using both *ab initio* and densityfunctional theory (DFT) calculations in *vacuo*.

2. Model and Numerical Method

We have employed self-consistent Hartree–Fock (HF) and DFT methods or the optimizationof geometries and energetic related to estimation of the structural variables for the dyads, namely, **1** and **2**. Thecalculationsare done using the SPARTAN'14 essential edition version. As these dyads contain more than 100 atoms,a smaller basis set is preferred to restrict the computation time. Therefore, themolecular structure is first optimized energetically to generate a stable structure using theHF/3-21G and B3LYP/3-21G levels of theory. Moreover, single point energy calculation is also performed for the dyads adding one more polarization function, i.e.,6-31G* at both HFand DFT calculations. This particular trick is being employed in view of the remarkable ability of B3LYP/6-31G*calculations to elucidate geometrical, electronic (and/ spectral)and electrochemical properties of the functionalized supramolecular dyad systems like porphyrin–fullereneensemble.26 The investigations on localization of molecular orbitals is done after the completion of optimization process as mentioned above. The electronic redistribution among various frontiermolecularorbitals, i.e.,lowestunoccupiedmolecular orbital (LUMO) and highest occupied molecular orbital (HOMO) always gives a direction by which photovoltaicproperties may be understood for any dyad systems.

3. Results and discussions

The optimized geometric structures of the dyads, namely, **1** and **2** using the HF/3-21G method are visualized in Figs. 1(a) & 1(b), respectively. The validity of HF/3-21G calculation for the elucidation of geometric structure and correct interpretation of the electronic structure for the non-covalently linked porphyrin-fullerene complex is already established by Nayak et al. [57] in which they have successfully explored the photophysical insights on a supramolecular recognition element consisting PyC_{60} and a bisporphyrin. In our present work, the bond distances between Zn atom and the nitrogen atoms of the porphyrin in dyad **2**

ranges from 1.93125Åto 2.09625Å. This structure is characterized in low spin state of zinc atom, which is supposed to be more favourable than the high spin state. It has been observed that in all the calculations as stated above, i.e., HF/3-21G, HF/6-31G* and DFT/B3LYP/6-31G*, the structural planarity is maintained in the dyad system **1**comprisingfree-base porphyrin and fulleropyrrolidine. However, slightly bending conformation is observedin the case of Zinc octaethylporphyrin-appended fulleropyrrolidine dyad**2**. The zinc atomis found to be protruded from the plane of the porphyrin molecule.The dihedral angles, namely,(C4,N1,Zn1,N2) and (C8,N2,Zn1,N1) obtained from DFT/B3LYP/6-31G* calculations are estimated to be 98.99° and 102.14°, respectively, which clearly signifies the difference of 3.15° between Zn1,N1 and Zn1,N2 linked conjugates. The center-to-centerdistancesbetween porphyrin and fullerenes in dyad **2** are computed to be 10.937Å, 11.336Å and 11.934Å as obtained from DFT, HF/6-31G* and HF/3-21G calculations, respectively. The center-to-center distance in case of dyad **1** is estimated to be somewhat higher, i.e., 13.315Å (as obtained from DFT calculations) compared to dyad **2**. This observation hints possibility of facile electron (and/ energy transfer) phenomenon in dyad **2** compared to dyad **1**. For dyad containing free-base porphyrin (i.e., **1**), the closest distance between 6:6 π-bond of fullerene with porphyrin and 6:6 carbon atom of fullerene with porphyrin are estimated to be 6.306Å and 6.877Å, respectively. In case of **2**, the said distances are calculated to be much less, i.e., 3.854Å (N1,Bond225) and 5.718Å(N1,C97), respectively. This observation clearly predicts that possibility of electron transfer and/ energy transfer is estimated to be much higher in case of **2** compared to **1**. Although in case of **1**, the distance between N atom of fulleropyrrolidine unit and N atom of porphyrin unit of free-base porphyrin is determined to be 15.098Å, it is estimated to be much less, i.e., 10.239Å in case of **2**. In present work, the possibility of C–H···π interaction in dyads **1** and **2** is also explored with the help of DFT calculations. C–H···πinteractionis established in case of Dyad

2between the 6-6 bond of fulleropyrrolidine unit (Bond 219) and the hydrogen atom (labelled as H8) of the porphyrin. The C–H····π distance is calculated to be 3.351Å. In case of **1**, C–H····π interaction exists between 6:6 π bond of fulleropyrrolidine unit (Bond marked as 216) and hydrogen atom (marked as H17) of poprhyrin subunit. The said distance is computed to be 3.854Å which is calculated to be ~0.5Å less compared to what is determined for **2**. The shorter distance of C–H····π interaction in case of dyad **2** reflects that ease of electron (and/ energy transfer) is facilitated in such conjugate system. Similar sort of phenomenon is also observed while estimating the distance between the α-pyrrole (i.e., porphyrin π-ring carbon) and one of [5,6] ring carbon atoms of fulleropyrrolidine (Por_{α}–Ful_{C}).The Por_{α}–Ful_{C} distances for dyad **1** and **2** are determined to be 4.584Å and 3.882Å, respectively.

The possibility of PET process in present work can be well understood in qualitative manner by inspecting the generated HOMO and LUMO pictures of dyads **1** and **2**. For exploring the charge-separated phenomenon in porphyrin–fulleropyrrolidine dyad(s), independent investigations are carried out on two major factors, *viz.*, the optimized structure of the porphyrin and fulleropyrrolidine moieties and the electronic nature of the spatialdistributionof frontier orbitals. Table 1 gives a comparison on the determined HOMOs and LUMOs for the optimized geometric structure of the dyads,e.g., **1** and **2** along with fulleropyyrolidine and porphyrinsforboth free-base and zincporphyrins. The HOMOs and LUMOs are calculated in different oxidation states ranging from n = 0 to n = 6 for HOMO – n and LUMO + n in case of free-base porphyrin, zincporphyrin, fulleropyrrolidine, **1** and **2**. Close inspection of Table 1 finds while LUMO energy level of dyad **1** is compared well with the fulleropyrrolidine unit (acceptor moiety), the HOMO energy level of dyad **2** corresponds well with that of porphyrin moiety. This disparity in observation may be explained due to the presence of divalent transition metal,Zn, in dyad **2**. Thorough scanning of the optimized geometric structures as depicted in Fig. 1, it is revealed while perfect planarity is maintained in **1** due to the flat

alignment of the porphyrin molecule, the out-of-plane alignment of the zinc atom in dyad **2**generatesdifferent types of electronic perturbations during the photoinduced ET process. Figs.2 and 3 show the corresponding diagrams ofthespatialdistribution of various HOMOs (*viz.*, HOMO, HOMO – 1, HOMO – 2, HOMO – 3, HOMO – 4& HOMO – 5)and LUMOs (*viz.*, LUMO, LUMO+1, LUMO+2, LUMO + 3, LUMO + 4 & LUMO + 5)energylevels of the dyad **1**, respectively, done by HF/3-21G calculations. Fig. 2 explores that position of HOMO is scattered between ethyl unit of porphyrin and corresponding linkage of fulleropyrrolidine-pyrrolidine conjugate in **1** (Fig. 2(a)). It is further observed that HOMO – 1 is precisely centered in porphyrin unit (Fig. 2(b)) and both the core part of HOMO – 2 (Fig. 2(c)) and HOMO – 3 (Fig. 2(d)) are evenly distributed among porphyrin and fulleropyrrolidine subunits of **1**. In case of **1**, complete positional change in terms of HOMO occurs from HOMO – 4 states, i.e., HOMO – 4 (Fig. 2(e))& HOMO – 5 (Fig. 2(f)). In case of various LUMOs, while LUMO is distributed among porphyrin and fulleropyrrolidine subunits of **1** (Fig. 3(a)), LUMO + 1 (Fig. 3(b)) & LUMO + 2 (Fig. 3(c)) are centered positioned in porphyrin subunit only.However, LUMO + 3 (Fig. 3(d)), LUMO + 4 (Fig. 3(e))& LUMO + 5 (Fig. 3(f)) states are precisely centered in fulleropyrrolidine subunit of **1** which actually signifies the decrement in extent of electron transfer upon irradiation by light. The scenario looks different in case of **2** if we compare the spatial distribution of various HOMOs and LUMOs at higher electronic states. In case of **2**, the corresponding positions of various HOMOs get interchanges between porphyrin and fulleropyrrolidine subunits which clearly states that extent of ET is very high upon irradiation by light in non-covalently linked dyad system.It is observed while HOMO (Fig. 4(a)), HOMO – 1 (Fig. 4(b)), HOMO – 2 (Fig. 4(c)), HOMO – 3 (Fig. 4(d)) & HOMO – 4 (Fig. 4(e)) are precisely positioned on porphyrin subunit of **2**, HOMO – 5 (Fig. 4(f)) may be located on fulleropyrrolidine unit. In case of distributions of various LUMOs, they are evenly distributed among poprhyrin and fulleropyrrolidine subunits in **2**. While Figs. 5(a), 5(b) &5(c) depict the positions of LUMO,

LUMO + 1 and LUMO + 2, respectively, LUMO + 3 (Fig. 5(d)), LUMO + 4 (Fig. 5(e)) & LUMO + 5 (Fig. 5(f)) states are centered on fulleropyrrolidine subunits of **2**.

This phenomenon proves that PET process is not supposed to occur spontaneously in case of **1** as revealed from the distribution of electronic charges over various frontier molecular orbitals. The scenario changes considerably when the spatial distributions of various HOMOs and LUMOs are studied for **2**. It is observed that HOMO to HOMO – n (when n = 1 to 4) states are precisely centered on fulleropyrrolidine unit in **2** (as revealed from Fig. 4). Only HOMO – 5 state is located in the porphyrin unit of **2**. Similar sort of observations are noticed while studying various LUMOs of **2**. While LUMO, LUMO + 1 and LUMO + 2 states are centered on porphyrin unit, LUMO + 3, LUMO + 4 and LUMO + 5 states are positioned on fulleropyrrolidine unit in **2**. Various LUMOs of **2** are demonstrated in Fig. 5.The above findings imply upon excitation by photoinduced process, theelectrontransfer process occurs from the porphyrin subunit to the fulleropyrrolidine subunit in **2**. Considering the optimized geometry and the electronic redistribution among various HOMOs and LUMOs in the porphyrin–fulleropyrrolidine dyads, a good understanding regarding localization of the excess charge in dyads **1** and **2** may be understood clearly in present work.TheMulliken charges for the dyads **1** and **2** are also evaluated in present investigations. Analysis of the charge distribution for the dyadsreveal that the localization of excess charge mainly occurs on fulleropyrrolidine subunit whilethe porphyrin subunit remains totally unaffected in case of localization of additional charge. This particular finding validates the mechanism of PET in dyads **1** and **2**. Like 3-21Gbasis set, we have made extensive quantum chemicalcalculationsof the dyads **1** and **2** employing 6-31G* basis set in B3LYPtechnique of calculations in both HF and DFT methods. The optimized space filling models of **1** and **2**in DFT/B3LYP/6-31G* calculations are visualized in Figs. 6&7, respectively. Table 2 summarizes the energies of the HOMO to HOMO – n and LUMO to LUMO + n states (where n = 6) of the dyad, namely, **2**doneby HF/6-31G*and DFT/B3LYP/6-31G*calculations. Table 2 indicates very small

energy gap between HOMO and LUMO as predicted by DFT/B3LYP/6-31G* calculations, i.e., 0.5074 which strongly hints efficient PET process for Dyad **2**. Table 3 summarizes the corresponding HOMO – LUMO energy gap (i.e., $E_{HOMO} - E_{LUMO}$) for both the dyads **1** and **2**computed by HF/3-21G calculations. The said calculations establish the lower energy gap in case of dyad **2** compared to dyad **1** which also substantiates the possibility of fast electron transfer in former system than that of later. One interesting observation of the present investigations is that the trend in $E_{HOMO} - E_{LUMO}$ for both **1** and **2**, *viz*., 1.3312 eV and 1.2079 eV, respectively, estimated by HF/3-21G calculations, corroborateexcellently well with those obtained from HF/6-31G* calculations. This phenomenon also points out that in spite of the absence of added polarization functions in HF/3-21G calculations, this particular computational model correctly predicts the possibility of PET in dyads **1** and **2**.

To find out the possibility of charge separation and to explore the feasibility of energy transfer phenomenon(a) from the free-base porphyrin and zincporphyrin units to fulleropyrrolidine unit in dyads **1** and **2**, respectively,different types of cartesian multipole moments have beengenerated in present investigations.The data of cartesian multipole moments for dyads **1** and **2** done by HF/6-31G* calculations are listed in Tables 4&5, respectively. As listed in Tables 4 & 5, it is very much evident that the dipole moment value of 39.2003 Debye for dyad **1** undergoes considerable increasewhen zinc metal is incorporated in the free-base porphyrin unit in Dyad **2**, i.e., 39.9911 Debye. This finding certainly proves that extent of charge-separation associated with photoinduced electron transfer is found to be much higher in case of dyad **2** compared to dyad **1**.

Calculation of the Mulliken charge distribution for the neutral dyad systems, i.e., **1** and **2**gives very good evidence in favour of facile PET in case of **2** compared to **1**. First of all, it is observed that the charge density is estimated to be higher on the fulleropyrrolidine subunit keepingthe porphyrin subunit unaffected. The determined value of average charge density over N atom in dyad**1** is -0.9366 a.u. which is estimated to be 0.1049 a.u. unit higher as

observed in case of**2**, *viz.,* -0.8317a.u. This observation proves that the N atoms of **2** donates electron at a much faster rate to the electron accepting fulleropyrrolidine unit during PET process. which This result validates the theory of the localization of the lowest unoccupied orbital on the acceptor side.

Calculations of molecular electrostatic potential(MEP) map of dyads **1** and **2** generate the regionsofboth positive and negative electrostatic potential at moderate to high level spreading over the donor and acceptor units.It iswell established that the strong electrostatic interactions persist between fullerene and porphyrin during non-covalent interaction which actually contributes major share of the total attractive interactions (i.e., ~60%) [68,69]. This result isin good corroboration with the fact that fullerenes have been employed as electron accepting species for constructing EDAtype complexes with various electron donors[70,71]. In recent past, Bichan et al. have contributed immensely for the exploration of supramolecular chemistry involving functionalized fullerene and various free-base porphyrins in solutions employing several spectroscopic tools [72-76]. Moreover, Ghanbari et al. have nicely demonstrated the spectroscopic and dispersion-corrected DFT study on robust fluorogenic non-porphyrin interaction of Zn(II) and Hg(II)naphthadiaza-crown macrocyclic complexes of C_{60}[77]. The same research group have made extensive photophysical, NMR and theoretical investigations on supramolecular dyad derived from a buckybowl series of O_2N_2-donor naphthodiaza-crowns coordinated to C_{60} [78].In a first report on supramolecular interaction of azobenzene moiety with C_{60}, Ghanbari et al. have studied in detail the binding of C_{60} in the cleft of new aza-crown macrocyclic tweezer tethered through an azobenzene linker [79].Close inspection of the MEP maps of both **1** (Fig. 8) and **2** (Fig. 9) done by HF/6-31G* calculations invoke that the fulleropyrrolidine unit in **2** gains predominant electron density(marked by dense red coloured dots)than that observed in **1** (mixed yellow and red coloured dots). Moreover, in case of **2**, there is no observation of red coloured dots in the center region of porphyrin unit

(as marked by deep green colouration in combination with yellow and blue mark). This observation proves that the porphyrin unit looseits electron density completely as a result of PET phenomenon to the fulleropyrrolidine unit in **2**. However, in case of **1**, other than combination of green and yellow colouration, some extents of red spots are seen. This means that the electron density is conserved at the center region of the porphyrin unit in **1** which actually indicates poor extent of PET phenomenon from the porphyrin unit to fulleropyrrolidine unit in the supramolecular entity. MEP clearly shows that surface of the fulleropyrrolidine unit gets shaded by deep red colour in **2** which indicates that significant amount of electric charge is transferred to such unit from zincporphyrin (Fig. 9). Generation of MEP also reveals that larger extent of positive electrostatic potential is clearly observed in the center region of the free-base porphyrin unit in **1** (Fig. 8)compared to **2**(Fig. 9) which ultimately gives very good support in favour of the strong PET phenomenon in later in comparison to former.

4. Conclusions

The geometric and electronic structures of two novel porphyrin–fulleropyrrolidine supamolecular dyads, **1** and **2**, have been explored in *vacuo* employing both *ab initio* and DFTcalculations. Various physicochemical parameters obtained from electronic structure give clear evidence in favour of spontaneous PET process in case of **2**. The possibility of photoinduced electron transportin these dyads are analyzedand explained on the basisofspatial distribution of various frontier orbitals, i.e. HOMO to HOMO – n and LUMO to LUMO + n (where n = 6). It is observed both the HOMO and LUMO suffer significant redistribution of electronic charges in dyads **1** and **2**. The analysis of Mulliken charge distribution and generation of molecular electrostatic potential maps providesa very good strategy by which the PET phenomena in the dyads can be understood. The present work nicely demonstrates that quantum chemical calculations at *ab initio* and DFT

levels of theorymay be successfully adopted to predict the excited-state ET pathway in non-covalently linked dyad systems.

5. Acknowledgments

SS thanks the authority of the University of Burdwan and Government of West Bengal for providing State Funded Fellowship to him. SB thanks CSIR, New Delhi for providing financial assistance through Research Project having Sanction No. **01/3083/21/EMR-II**.

Declarations

Ethical Approval

Not applicable.

Competing interests

The authors declare no competing as well as conflict of interest in this work.

Authors' contributions

Shalmali Bhattacharya, Shiv Sankar Saha and Subrata Nayak have performed the work of all computational calculations. Dr. S. Chatterjee has done the graphical work. The paper is compiled and written by Prof. S. Bhattacharya and Dr. S. Banerjee.

Funding

The present research work gets financial assistance through CSIR Research Project having Sanction No. 01(3083)/21/EMR-II.

Availability of data and materials

Availability of data sets and their access can be obtained directly from the authors as and when required.

References:

1. G. Suneel, K. Jain, B. Anjaiah, H. Mitra, R. A. Ramnagar, S. Bandi, V. Chuncha, T. K. Roy, L. Giribabu, R. Chitta, Light-induced energy and electron transfer occurring in tandem in tetra (bis(4′-tert-butylbiphenyl-4-yl)aniline)-zinc(II) porphyrin-fullerene supramolecular conjugates, Journal of Porphyrin and Phthalocyanine, 26 (2022) 872-883.

2. Wong K -T, Bassani DM, (2014) Energy transfer in supramolecular materials for new applications in photonics and electronics (2014) NPG Asia Materials, 6:e116.

3. Santoro A, Bella G, Cancelliere AM, Serroni S, Lazzaro G, Campagna S, Photoinduced Electron Transfer in Organized Assemblies—Case Studies (2022), Molecules, 27:2713.

4. Yu X, Wang B, Kim Y, Park J, Ghosh S, Dhara B, Mukhopadhyay RD, Koo J, Kim I, Kim S, Hwang I -C, Seki S, Guldi DM, Baik M -H, Kim K, Supramolecular Fullerene Tetramers Concocted with Porphyrin Boxes Enable Efficient Charge Separation and Delocalization, JACS, 142: 12596-12601.

5. Armaroli N, Photoinduced Energy Transfer Processes in Functionalized Fullerenes, Book Chapter 5 in Fullerenes: From Synthesis to Optoelectronic Properties, (2022): 137-162.

6. Karla A. Ortiz-Soto, Oscar A. Jaramillo-Quintero, Edgar Alvarez-Zauco, Marina E. Rincon, Charge Transfer in Self-Assembled Fullerene-Tetraphenylporphyrin Non-Covalent Multilayer, ECS Journal of Solid State Science and Technology (2022) 11:014001.

7. Mondol P, Rath SP,Cyclic Metalloporphyrin Dimers: Conformational Flexibility, Applications and Future Prospects,Coord. Chem. Rev. (2020), 405: 213117.

8. Jha A, Sankar H, Kumar S, Sankar M, Kar P,Efficient charge transfer from organometal lead halide perovskite nanocrystals to free base meso -tetraphenylporphyrins, Nanoscale Advances. (2022) 4: 1779–1785**.**

9. Franco MA, Groesser SN, A Systematic Literature Review of the Solar Photovoltaic Value Chain for a Circular Economy (2021) 13: 9615.

10. Alharbi FH, Kais S,Theoretical limits of photovoltaics efficiency and possible improvements by intuitive approaches learned from photosynthesis and quantum coherence, Renewable and Sustainable Energy Reviews (2015) 43:1073-1089.

11. Bottari G, Torre GDL, Torres T, Covalent and Noncovalent Phthalocyanine-Carbon Nanostructure Systems: Synthesis, Photoinduced Electron Transfer, and Application to Molecular Photovoltaics, Chem. Rev. (2010) 110: 6768.

12. Ji W, W T -X, Ding X, Lei S, Han B -H,Porphyrin- and phthalocyanine-based porousorganic polymers: From synthesis to application (2021) Coord. Chem. Rev. 439:213875.

13. Handbook of Porphyrin Science: With Applications to Chemistry, Physics, Materials Science, Engineering, Biology and Medicine — Volume 46: Modern Aspects of Porphyrinoid Chemistry, Edited By: Kadish KM, Smith KM, Guilard R, World Scientific, (2022) Pages: 376.

14. Hou L, Cui X, Guan B, Wang S, Li R, Liu Y, Zhu D, Zheng J, Synthesis of a monolayer fullerene network, Nature (2022) 606: 507-510.

15. Yamada M, Kurihara Y, Koizumi M, Tsuji K, Maeda Y, Suzuki M, Understanding the Nature and Strength of Noncovalent Face-to-Face Arene–Fullerene Interactions, Angew. Chem. Int. Ed. (2022) 61.

16. Kroto HW, Heath JR, O'Brien SC, Curl RF, Smalley RE, C_{60}: Buckminsterfullerene, Nature (1985) 318: 162-163.

17. Mateo-Alonso A, Guldi DM, Paolucci F, Prato M, Fullerenes: Multitask Components in Molecular Machinery, Angew. Chem. Int. Ed. (2007) 46: 8120 – 8126.

18. Wang Y, Photophysical properties of fullerenes and fullerene/N,N-diethylaniline charge-transfer complexes, J. Phys. Chem. (1992) 96: 764-767.

19. Nilolaou V, Charisiadis A, Stangel C, Charalambidis G, Coutsolelos AG, Porphyrinoid–Fullerene Hybrids as Candidates in Artificial Photosynthetic Schemes, C (2019) 5:53.

20. Caballero C, Calbo J, Arago J, Cruz PDL, Orti E, Tkachenko NV, Langa F, Enhanced electronic communication through a conjugated bridge in a porphyrin–fullerene donor–acceptor couple, Journal of Materials Chemistry C (2021) 9: 10889-10898.

21. Wessendorf F, Grimm B, Guldi DM, Hirsch A, Pairing Fullerenes and Porphyrins: Supramolecular Wires That Exhibit Charge Transfer Activity, J. Am. Chem. Soc. (2010) 132: 10786-10795.

22. Jozeliunaite A, Neniskis A, Bertran A, Bowen AM, Valentin MD, Raisys S, Baronas P, Kazlauskas K, Vilciauskas L, Orentas E, Fullerene Complexation in a Hydrogen-Bonded Porphyrin Receptor via Induced-Fit: Cooperative Action of Tautomerization and C–H···π Interactions, J. Am. Chem. Soc. (2023) 145: 455-464.

23. Porcu P, Estrada-Montaño AS, Vonlanthen M, Cuétara-Guadarrama F, González-Méndez I, Sorroza-Martínez K, Zaragoza-Galán G, Rivera E,Azobenzene dyads containing fullerene, porphyrin and pyrene chromophores: Molecular design and optical properties, Dyes and Pigments (2022) 197: 109858.

24. Liu L, Chen X, Chai Y, Zhang W, Liu X, Zhao F, Wang Z, Weng Y, Wu B, Geng H, Zhu Y, Wang C,Highly efficient photocatalytic hydrogen production via porphyrin-fullerene supramolecular photocatalyst with donor-acceptor structure, Chemical Engineering Journal (2022) 444: 136621.

25. Ray A, Bhattacharya S, Molecular complexation between PCBM and porphyrazine in solution: A case study of non-covalent interaction, J. Mol. Liq. (2018) 254:291.

26. Y. Xu, B. Wang, M.B. Minameyer, M. Bothe, T. Drewello, D.M. Guldi, M.V. Delius, A Supramolecular [10]CPP Junction Enables Efficient Electron Transfer in Modular Porphyrin–[10]CPP⊃Fullerene ComplexesAngew. Chem. Int. Ed. (2018) 57: 11549–11553.

27. Ray A, Banerjee S,Ghosh S, Bauri AK, Bhattacharya S, Chemical physics behind formation of efficientcharge separated state ofcomplexation between $PC_{70}BM$ and designed diporphyrin in solution, Spectrochim. Acta part A (2016) 152:64.

28. G.M. Gedda, G.U. Kulkarni, S.S. Babu, One-Dimensional Porphyrin–Fullerene (C_{60}) Assemblies: Role of Central Metal Ion in Enhancing Ambipolar MobilityChem. Eur. J. (2018) 24: 7695–7701.

29. Ray A, Banerjee S, Bauri AK, Bhattacharya S, Chemical physics behind formation of effectiveand selective non-covalent interactionbetween fullerenes (C_{60} and C_{70}) and a designedchiral monoporphyrin insolution, Chem. Phys. Lett. (2016) 646:119.

30. D.V. Konarev, S.S. Khasanov, R.N. Lyubovskaya, Fullerene complexes with coordination assemblies of metalloporphyrins and metal phthalocyaninesCoord. Chem. Rev. (2014) 262: 16–36.

31. Ray A, Bauri A, Bhattacharya S, Absorptionspectrophotometric,fluorescence and quantum chemicalinvestigations on non-covalent interactionbetween $PC_{70}BM$ anddesigned diporphyrin insolution, (2015) 134:566.

32. M. Takeda, S. Hiroto, H. Yokoi, S. Lee, D. Kim, H. Shinokubo, Azabuckybowl-Based Molecular Tweezers as C_{60} and C_{70} Receptors, J. Am. Chem. Soc. (2018) 140: 6336–6342.

33. Ghosh BK, Bauri A, Bhattacharya S, Banerjee S, Photophysical investigations oneffective and selectivecomplexation of adesigned monoporphyrin with C_{60} and C_{70} insolution, Spectrochim. Acta part A (2014) 125:90.

34. S. Fukuzumi, K. Ohkubo, T. Suenobu, Long-Lived Charge Separation and Applications in Artificial Photosynthesis, Acc. Chem. Res. (2014) 47: 1455–1464.

35. Otsuki J, Supramolecular approach towards light-harvesting materials based on porphyrins and chlorophylls, J. Mater. Chem. A (2018) 6: 6710-6753.

36. Hashikawa Y, Sadai S, Okamoto S, Murata Y, Near-Infrared-Absorbing Chiral Open [60]Fullerenes, Angew. Chem. Int. Ed. (2023) 62.

37. Bhattacharya S, Nayak S K, Chattopadhyay S K, Banerjee M, Mukherjee A K, Absorptionspectroscopicstudy of EDA complexesof [70]fullerene with aseries of methyl Benzenes, Spectrochim. Acta part A (2001) 57: 309.

38. Bhattacharya S, Banerjee M, Mukherjee A K, Study of the formationequilibria of theformation equilibria ofelectron donor-acceptorcomplexes between [60]fullerene andmethylbenzenes byabsorption spectrometricmethod, Spectrochim. Acta part A (2001) 57: 1463.

39. Bhattacharya S, Nayak S K, Chattopadhyay S, Banerjee M, Mukherjee A K, Spectrophotometric andthermodynamic study ofsupramolecularcomplexes of [60] and[70]fullerenes with anumber ofcalix[n]arenes, J. Chem. Soc. Perkin Trans. 2 (2001) 2292.

40.Lecture Notes on Fullerene Chemistry: A Handbook for ChemistsBy Taylor R, World Scientific (1999) Pages: 288.

41. Imahori H, Fukuzumi S, Porphyrin- and Fullerene-Based Molecular Photovoltaic Devices Advanced Functional Materials (2004) 14.

42. Llansola-Portoles M J, Gust D, Moore T A, Moore A L, Artificial photosynthetic antennas and reaction centers, ComptesRendus Chimie (2017) 20: 296-313.

43. Imahori H, Porphyrin–fullerene linked systems as artificial photosynthetic mimics, Org. Biomol. Chem. (2004) 2: 1425–1433.

44. Lyubov A F, Furmansky Y, Shestakov A F, Emelianov N A, Liddell P A, Gust D, Visoly-Fisher I, Troshin P A, Advanced Nonvolatile Organic Optical Memory Using Self-Assembled Monolayers of Porphyrin–Fullerene Dyads, ACS Appl. Mater. Interfaces (2022) 14: 15461–15467.

45. Stasyuk A J, Stasyuk O A, Solà M, Voityuk A A, Peculiar Photoinduced Electron Transfer in Porphyrin–Fullerene Akamptisomers, Chemistry A European Journal (2019) 25: 2577-2585.

46. Kausar A, Ahmad I, Maaza M, Eisa M H, Bocchetta P, Polymer/Fullerene Nanocomposite for Optoelectronics—Moving toward Green Technology, J. Compos. Sci. (2022) 6: 393.

47. Rabiee N, Yaraki M T, Garakani S M, Garakani S M, Ahmadi S, Lajevardi A, Bagherzadeh M, Rabiee M, Tayebi L, Tahriri M, Hamblin M R, Recent Advances in Porphyrin-Based Nanocomposites for Effective Targeted Imaging and Therapy, Biomaterials (2020) 232: 119707.

48.Sessler J L, Tvermoes N A, Davis J, Anzenbacher P, Jursíková K, Sato W, Seidel D, Lynch V, Black C, Try A, Andrioletti B, He mmiG, Mody T D, Magda D J, Král V, Pure and Applied Chemistry (1999) 71: 2009-2018.

49. Gupta N, Sharma C, Kumar M, Kumar R, Synthesis and comparative charge transfer studies in porphyrin–fullerene dyads: mode of attachment effect, New J. Chem. (2017) 41: 13276.

50. Tkachenko N, Efimov A, Lemmetyinen H, Porphyrin-Based Donor–Acceptor Dyads — Engineering the Linker and Tuning the Photoinduced Electron Transfer, (2016) 121: 171.

51. Grover N, Chaudhri N, Sankar M,*β*-substituted donor-acceptor porphyrins: Synthesis, energy transfer and electrochemical redox properties, Dyes and Pigments, (2019) 161: 104-112.

52. Porcu P, Estrada-Montaño A S, Vonlanthen M, Cuétara-Guadarrama F, González-Méndez I, Sorroza-Martínez K, Zaragoza-Galán G, Rivera E, Azobenzene dyads containing fullerene, porphyrin and pyrene chromophores: Molecular design and optical properties, Dyes and Pigments, (2022) 197: 109858.

53. Sissaoui, J, Efimov A, Kumpulainen T, Vauthey E. Photoinduced Electron Transfer in a Porphyrin-Fullerene Dyad at a Liquid Interface, Journal of Physical Chemistry B, (2022)26: 4723-4730.

54. Stangel C, Plass F,Charisiadis A,Giannoudis E,Chararalambidis G, Karikis K, Rotas G,Zervaki GE,Lathiotakis NN, Tagmatarchis N et al. Interfacing tetrapyridyl-C-60 with porphyrin dimers via -conjugated bridges: artificial photosynthetic systems with ultrafast charge separationPhys. Chem. Chem. Phys (2018)20:21269–21279.

55. Lyubov A. Frolova, Yulia Furmansky, Alexander F. Shestakov, Nikita A. Emelianov, Paul A. Liddell, Devens Gust, Visoly-Fisher I, Troshin P A, AdvancedNonvolatile Organic Optical Memory Using Self-Assembled Monolayers of Porphyrin–Fullerene Dyads, ACS Appl Mater Interfaces (2022) 14: 15461–15467.

56. Tkachenko N V, Effect of the Donor/Acceptor Size on the Rate of Photo-Induced Electron Transfer, Photochem(2022) 2: 918–931.

57. Nayak S, Ray A, Bhattacharya S, Bauri A, Banerjee S, Photophysical insights on a new supramolecular recognition element comprising PyC_{60} and a bisporphyrin studied in solution, J. Mol. Liq. (2019) 290: 110842.

58. S.K. Das, B. Song, A. Mahler, V.N. Nesterov, A.K. Wilson, O. Ito, F. D'Souza, Electron transfer studies of high potential zinc porphyrin–fullerene supramolecular dyads, J. Phys. Chem. C 118 (2014) 3994–4006.

59. L. Moreira, J. Calbo, J. Aragó, B.M. Illescas, I. Nierengarten, B. Delavaux-Nicot, E. Ortí, N. Martín, J.-F. Nierengarten, Electron transfer studies of high potential zinc porphyrin–fullerene supramolecular dyads, J. Am. Chem. Soc. 138 (2016) 15359–15367.

60. M. Ortiz, S. Cho, J. Niklas, S. Kim, O.G. Poluektov, W. Zhang, G. Rumbles, J. Park, Through-Space Ultrafast Photoinduced Electron Transfer Dynamics of a C_{70}-Encapsulated Bisporphyrin Covalent Organic Polyhedron in a Low-Dielectric Medium, J. Am. Chem.Soc. 139 (2017) 4286–4289.

61. M.E. El-Khouly, L.M. Rogers, M.E. Zandler, G. Suresh, M. Fujitsuka, O. Ito, F. D'Souza, Studies on Intra-Supramolecular and Intermolecular Electron-Transfer Processes between Zinc Naphthalocyanine and Imidazole-Appended Fullerene, Chem. Phys. Chem. 4 (2003) 474–481.

62. S. Nayak, S. Paul, A. Bauri, A. Ray, S. Bhattacharya, Molecular assembly of $PC_{70}BM$ with a designed monoporphyrin: Spectroscopic investigation in solution and theoretical calculations, J. Mol. Liq. 272 (2018) 137–150.

63. A. Ray, S. Bhattacharya, Photophysical insights behind zinc naphthalocyanine-gold nanoparticle interaction and its effect over supramolecular interaction between zinc napthalocyanine and PyC_{60} in solution, J. Mol. Liq. 232 (2017) 188–194.

64. M. Wielopolski, A. Molina-Ontoria, C. Schubert, J. Margraf, E. Krokos, J. Kirschner, A. Gouloumis, T. Clark, D.M. Guldi, N. Martín, Blending Through-Space and Through-Bond π–π-Coupling in [2,2′]-Paracyclophane-oligophenylenevinylene Molecular Wires J. Am. Chem. Soc. 135 (2013) 10372–10381.

65. K.A. Nielsen, W.-S. Cho, G.H. Sarova, B.M. Petersen, A.D. Bond, J. Becher, F. Jensen, D.M. Guldi, J.L. Sessler, J.O. Jeppesen, Supramolecular Receptor Design: Anion-Triggered Binding of $C_{60,}$ Angew. Chem. Int. Ed. 45 (2006) 6848–6853.

66. D. Pal, K. Kundu, S.K. Nayak, S. Bhattacharya, PyC_{60}-naphthacrown system: A new supramolecular recognition element, Spectrochim. Acta Part A 138 (2015) 958–963.

67. S. Nayak, A. Ray, S. Bhattacharya, Size selective supramolecular interaction upon molecular complexation of a designed porphyrin with C_{60} and C_{70} in solution, J. Mol. Liq. 321 (2021) 114367.

68. Y.-B. Wang, Z. Lin, Supramolecular Interactions between Fullerenes and Porphyrins, J. Am. Chem. Soc.125 (2003) 6072-6073.

69. D.R. Evans, N.L.P Fackler, Z. Xie, C.E.F. Rickard, P.D.W. Boyd, C.A. Reed, π-Arene/Cation Structure and Bonding. Solvation versus Ligand Binding in Iron(III) Tetraphenylporphyrin Complexes of Benzene, Toluene, *p*-Xylene, and [60]Fullerene J. Am. Chem. Soc. 121 (1999) 8466-8474.

70. A. Ray, D. Goswami, S. Chattopadhyay, S. Bhattacharya, Photophysical and Theoretical Investigations on Fullerene/Phthalocyanine Supramolecular Complexes, J. Phys. Chem. A 112 (2008) 11627-11640.

71. A. Ray, K. Santhosh, S. Bhattacharya, New Photophysical Insights in Noncovalent Interaction between Fulleropyrrolidine and a Series of Zincphthalocyanines J. Phys. Chem. A 115 (2011) 9929-9940.

72. N.G.Bichan, E. N. Ovchenkova, V. A.Mozgova, N. O.Kudryakova, T. N.Lomova, Three cobalt(II) porphyrins ligated with pyridyl-containing nanocarbon/gold(III) porphyrin for solar cells: Synthesis and characterization, Polyhedron,203 (2021) 115223.

73. N. G. Bichan, E. N.Ovchenkova, V. A.Mozgova, N. O.Kudryakova, M. S. Gruzdev, T. N. Lomova, Mechanism of the Self-Assembly of Donor–Acceptor Triads Based on Cobalt(II) Porphyrin Complex and Fullero[60]pyrrolidine, According to Data Obtained by Spectroscopic and Electrochemical Means, J. Phys. Chem. A, 94 (2020) 1159–1166.

74. N. G. Bichan, E. N.Ovchenkova, V. A.Mozgova, N. O.Kudryakova, T. N.Lomova, Formation Reaction, Spectroscopy, and Photoelectrochemistry of the Donor–Acceptor Complex (5,10,15,20-Tetraphenyl-21,23H-porphinato)cobalt(II) with Pyridyl-Substituted Fullero[60]pyrrolidine, Russ. J. Inorg. Chem. 64 (2019) 605–614.

75. N. G. Bichan, E. N.Ovchenkova, M. S. Gruzdev, T. N.Lomova, Chemical Structure of Pyridine Complexes Of Oxo(5,10,15,20-Tetraphenyl-21H,23H-Porphinato) Niobium(V) Chloride According to Formation Thermodynamics/Kinetics And Spectroscopy Data, J. Struct. Chem. 59 (2018) 711–719.

76. N. G. Bichan, E. N. Ovchenkova, V. A. Mozgova, A. A. Ksenofontov, N. O. Kudryakova, I. V. Shelaev, F. E. Gostev, T. N. Lomova, Molecules, Donor–Acceptor Complexes of (5,10,15,20-Tetra(4-methylphenyl)porphyrinato)cobalt(II) with Fullerenes C_{60}: Self-Assembly, Spectral, Electrochemical and Photophysical Properties, 27(2022) 8900.

77. B. Ghanbari, M.Zarepour-jevinani, A. H. Mohammadzadeh, Robust Fluorogenic Non-porphyrin Interaction of Zn(II) and Hg(II) Naphthadiaza-crown Macrocyclic Complexes with C60: Spectroscopic and Dispersion-corrected DFT Study, Journal of Photochemistry & Photobiology, A: Chemistry 418 (2021) 113414.

78. B. Ghanbari, M. Zarepour-jevinani, Supramol. Chem. Supramolecular dyad derived from a buckybowl series of O_2N_2-donor naphthodiaza-crowns coordinated to C_{60}: photophysical, NMR and theoretical studies, 29 (2017) 248-258.

79. B. Ghanbari, M.Mahdavian, A.M. García-Deibe, Synthesis and photoisomerization study of new aza-crown macrocyclic tweezer tethered through an azobenzene linker: The first report on supramolecular interaction of azobenzene moiety with C_{60}, J. Mol. Struct. 1144 (2017) 360-369.

Table 1. Comparison of the seven highest occupied and seven lowest unoccupied molecular orbital levels of free-base porphyrin, zincporphyrin, N-methylfulleropyrrolidine, **1** and**2** done by HF 3-21G calculation.

	Energy, eV				
Frontier Orbitals	Free-base porphyrin	Zincporphyrin	N-methylfulleropyrrolidine	**1**	**2**
HOMO – 6	-13.0884	-12.0592	-9.6131	-7.3376	-7.2675
HOMO – 5	-12.9224	-11.6008	-9.2695	-7.1909	-7.0086
HOMO – 4	-12.4225	-11.3323	-8.6110	-7.1190	-6.5396
HOMO – 3	-12.3164	-11.2367	-8.1557	-6.9993	-6.3275
HOMO – 2	-11.4525	-11.0186	-8.0304	-6.9665	-6.2766
HOMO – 1	-10.2019	-9.3596	-8.0095	-6.6858	-6.0519

HOMO	-9.7948	-8.5517	-7.7714	-4.3925	-4.4229
LUMO	-3.1682	-4.4330	-0.6498	-3.0613	-3.2150
LUMO + 1	-1.6102	-1.8446	-0.4262	-0.2355	-0.3242
LUMO + 2	-0.5987	-1.3685	-0.1277	-0.0560	0.1026
LUMO + 3	1.4414	0.9313	1.0541	0.9409	1.0556
LUMO + 4	2.3977	1.5975	1.2795	1.2859	1.5672
LUMO + 5	3.3446	2.1347	1.5253	1.7143	1.9753
LUMO + 6	3.4435	2.5843	1.6310	2.4064	2.4115

Table 2. Energies of the HOMO to HOMO – n and LUMO to LUMO + n states (where n = 6) of the dyad, namely, **2** done by HF/6-31G* and B3LYP/6-31G* calculations.

	Energy, eV	
	Method	
	HF/6-31G*	**DFT/B3LYP/6-31G***
Frontier Orbitals	**2**	**2**
HOMO – 6	-8.6278	-7.3894
HOMO – 5	-8.4588	-7.3582
HOMO – 4	-7.9039	-7.2415
HOMO – 3	-7.6917	-7.2176
HOMO – 2	-7.6387	-6.4502

HOMO – 1	-7.4262	-6.8430
HOMO	-5.8834	-5.6619
LUMO	-4.3253	-5.1545
LUMO + 1	-1.8945	-4.1267
LUMO + 2	-1.4885	-3.9415
LUMO + 3	-0.4320	-3.6473
LUMO + 4	0.0696	-3.6097
LUMO + 5	0.4880	-3.5738
LUMO + 6	0.9444	-3.0987

Table 3. HOMO – LUMO energy gap of dyads **1** and **2** computed by HF/3-21G calculations.

Method	HOMO – LUMO Energy gap, eV	
	1	**2**
HF/3-21G	1.3312	1.2079

Table 4. Multipole moments of dyad **2** done by HF/6-31G* calculations.

```
-------------------------------------------------------------
Cartesian Multipole Moments
-------------------------------------------------------------
Charge (ESU x 10^10)
0.0000
Dipole Moment (Debye)
X 35.9543 Y 15.3184 Z -3.0496
Tot 39.2003
Quadrupole Moments (Debye-Ang)
XX -355.8379 XY 116.9420 YY -455.9307
XZ -8.1303 YZ -9.5805 ZZ -607.4487
Traceless Quadrupole Moments (Debye-Ang)
QXX 351.7036 QYY 51.4253 QZZ -403.1288
QXY 350.8260 QXZ -24.3910 QYZ -28.7415
```

```
Octapole Moments (Debye-Ang^2)
XXX 3097.7732 XXY 1009.2518 XYY 1347.4578
YYY 650.8150 XXZ -122.5569 XYZ -109.5456
YYZ -138.3737 XZZ 157.6608 YZZ 42.5093
ZZZ -39.2813
Traceless Octapole Moments (Debye-Ang^2)
XXX 5040.5721 YYY -5560.9604 ZZZ 2112.6875
XXY 10031.0488 XXZ -937.7180 XYY 6403.1918
XYZ -1643.1847 XZZ -11443.7640 YYZ -1174.9695
YZZ -4470.0884
Hexadecapole Moments (Debye-Ang^3)
XXXX -116810.5967 XXXY 8505.9333 XXYY -19805.4411
XYYY 4885.5623 YYYY -20152.0966 XXXZ -100.6975
XXYZ -677.8820 XYYZ -877.2009 YYYZ -524.8518
XXZZ -26381.5687 XYZZ 169.7613 YYZZ -5896.8262
XZZZ 284.5214 YZZZ -67.4764 ZZZZ -10739.1510
Traceless Hexadecapole Moments (Debye-Ang^3)
XXXX 137846.2833 XXXY 282866.4372 XXXZ 20628.7283
XXYY 297599.6938 XXYZ -52131.6031 XXZZ -435445.9771
XYYY -97272.5243 XYYZ -81705.4419 XYZZ -185593.9129
XZZZ 61076.7137 YYYY -255903.0422 YYYZ 2028.5834
YYZZ -41696.6516 YZZZ 50103.0197 ZZZZ 477142.6287
-----------------------------------------------------------------
```

Table 5. Multipole moments of dyad **2** done by HF/6-31G* calculations.

```
-----------------------------------------------------------------
Cartesian Multipole Moments
-----------------------------------------------------------------
Charge (ESU x 10^10)
0.0000
Dipole Moment (Debye)
X 29.4632 Y 25.7516 Z -8.2499
Tot 39.9911
Quadrupole Moments (Debye-Ang)
XX -456.6386 XY 66.6075 YY -463.0515
XZ -92.3811 YZ -67.8116 ZZ -494.7054
Traceless Quadrupole Moments (Debye-Ang)
QXX 44.4797 QYY 25.2409 QZZ -69.7206
QXY 199.8226 QXZ -277.1434 QYZ -203.4347
Octapole Moments (Debye-Ang^2)
XXX 1153.5651 XXY 707.2492 XYY 642.5808
YYY 542.8483 XXZ -424.9718 XYZ -373.4294
YYZ -208.5000 XZZ 619.9573 YZZ 307.4270
ZZZ -185.5094
Traceless Octapole Moments (Debye-Ang^2)
XXX -4441.4530 YYY -5874.9964 ZZZ 4588.1891
XXY 5936.1649 XXZ -3917.6330 XYY 2390.4028
XYZ -5601.4416 XZZ 2051.0502 YYZ -670.5560
YZZ -61.1684
Hexadecapole Moments (Debye-Ang^3)
```

```
XXXX -41307.5873 XXXY 2771.9984 XXYY -8928.1738
XYYY 871.5531 YYYY -24991.8185 XXXZ -3092.2885
XXYZ -2260.0719 XYYZ -1674.3449 YYYZ -1194.0373
XXZZ -9291.9835 XYZZ 1343.8204 YYZZ -7071.3655
XZZZ -1372.0816 YZZZ -1061.8838 ZZZZ -20604.0302
Traceless Hexadecapole Moments (Debye-Ang^3)
XXXX -217177.9895 XXXY 66628.0954 XXXZ -48448.1180
XXYY 157868.8444 XXYZ -169580.9097 XXZZ 59309.1451
XYYY -132918.6605 XYYZ -83725.4913 XYZZ 66290.5651
XZZZ 132173.6093 YYYY -172297.0748 YYYZ 77805.9951
YYZZ 14428.2305 YZZZ 91774.9146 ZZZZ -73737.3756
-----------------------------------------------------------------
```

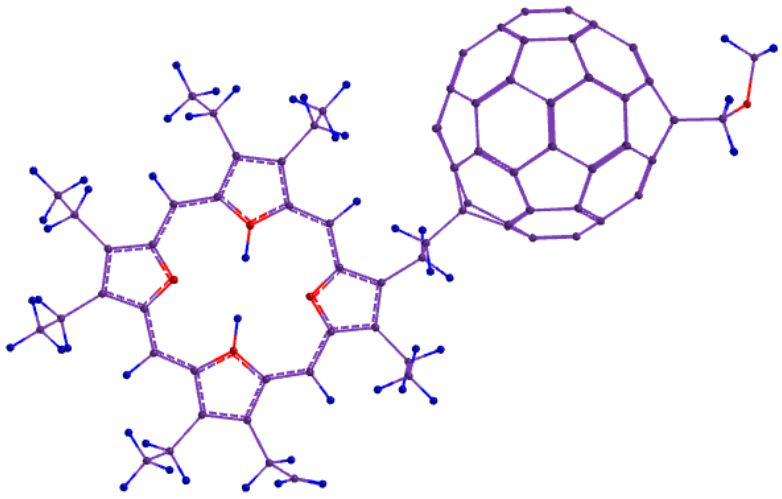

(a)

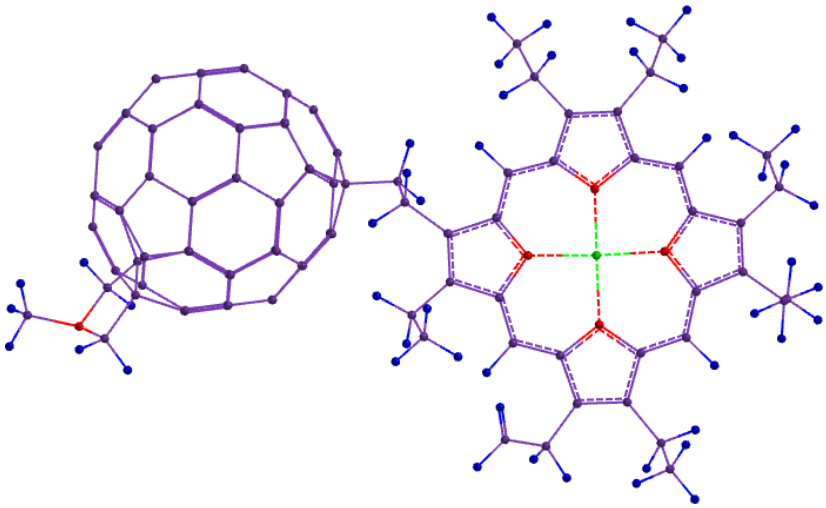

(b)

Fig. 1. Geometric structures of (a) **1** and (b) **2** done by HF/3-21G calculations.

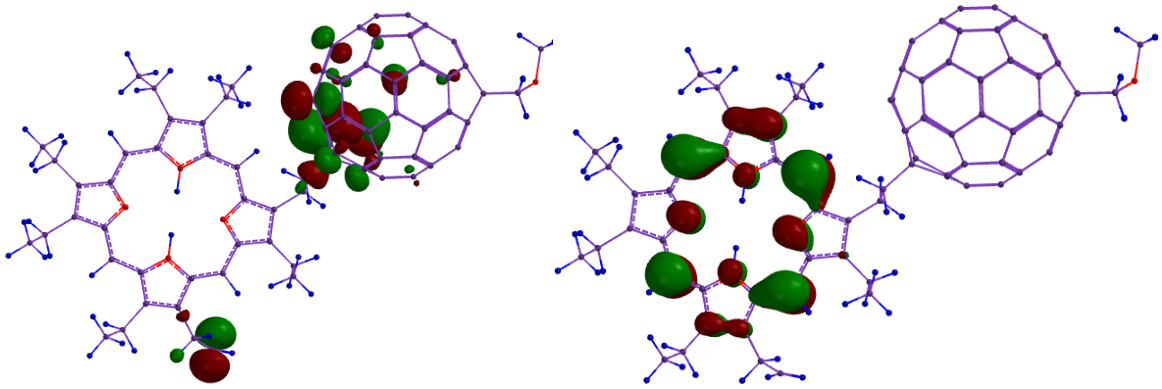

(a) (b)

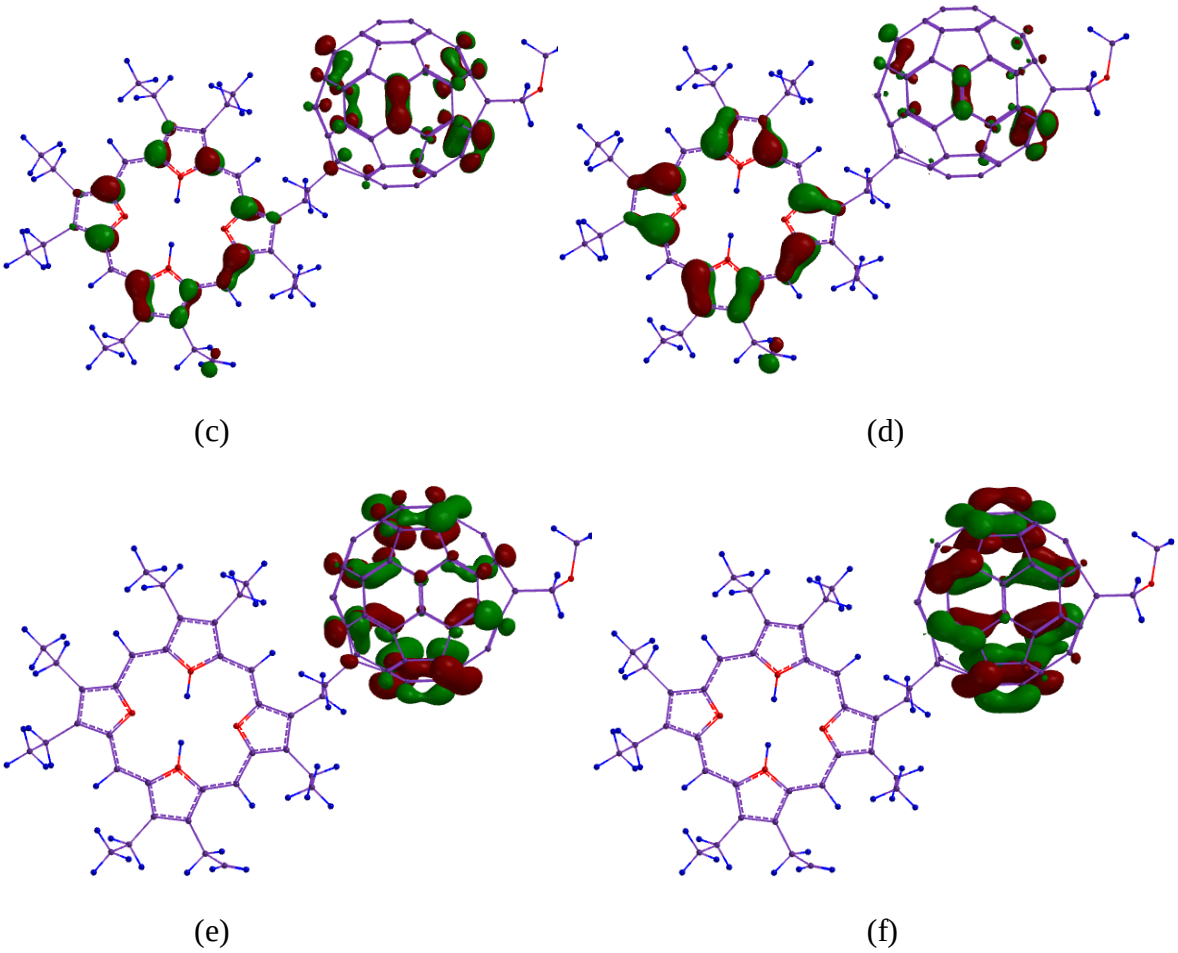

(c) (d)

(e) (f)

Fig. 2. (a) HOMO, (b) HOMO – 1, (c) HOMO – 2, (d) HOMO – 3, (e) HOMO – 4 and (f) HOMO – 5 states of dyad **1** done by HF/3-21G calculations.

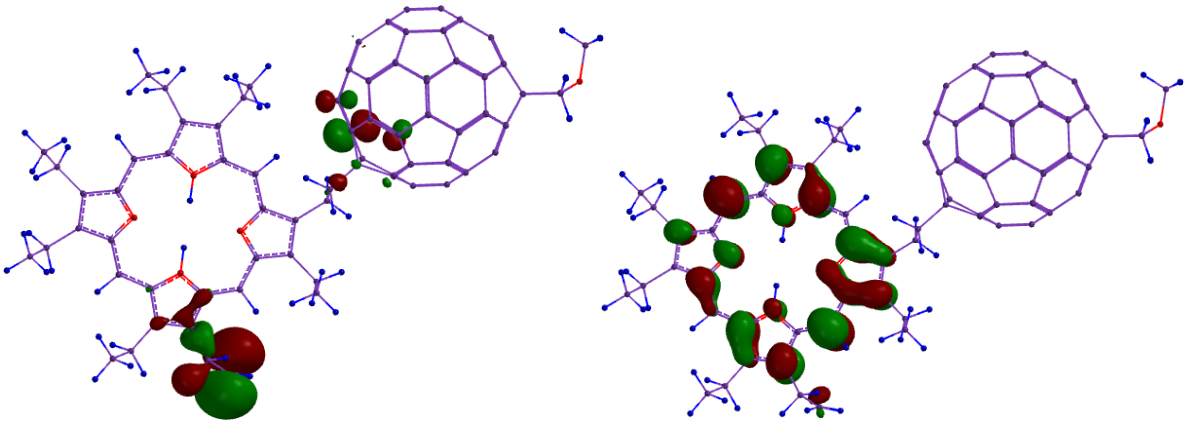

(a) (b)

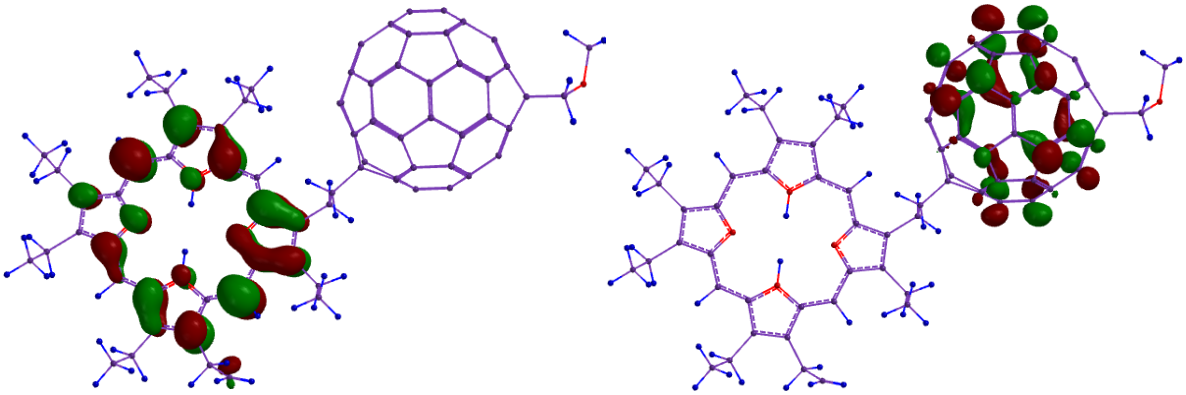

(c) (d)

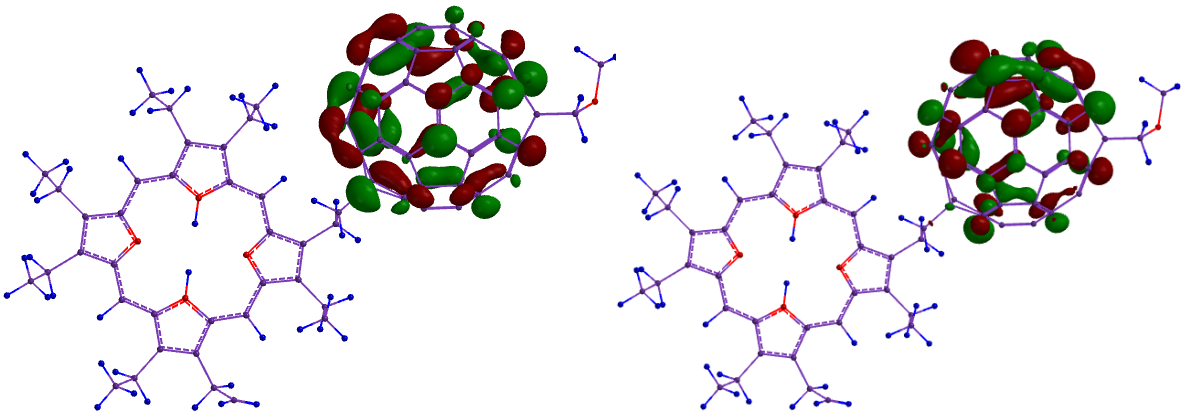

(e) (f)

Fig. 3. (a) LUMO, (b) LUMO + 1, (c) LUMO + 2, (d) LUMO + 3, (e) LUMO + 4 and (f) LUMO + 5 states of dyad **1** done by HF/3-21G calculations.

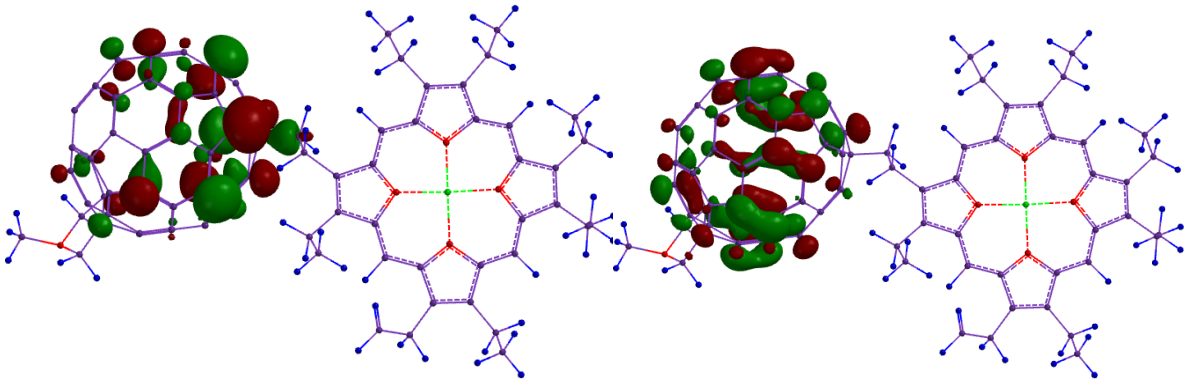

(a) (b)

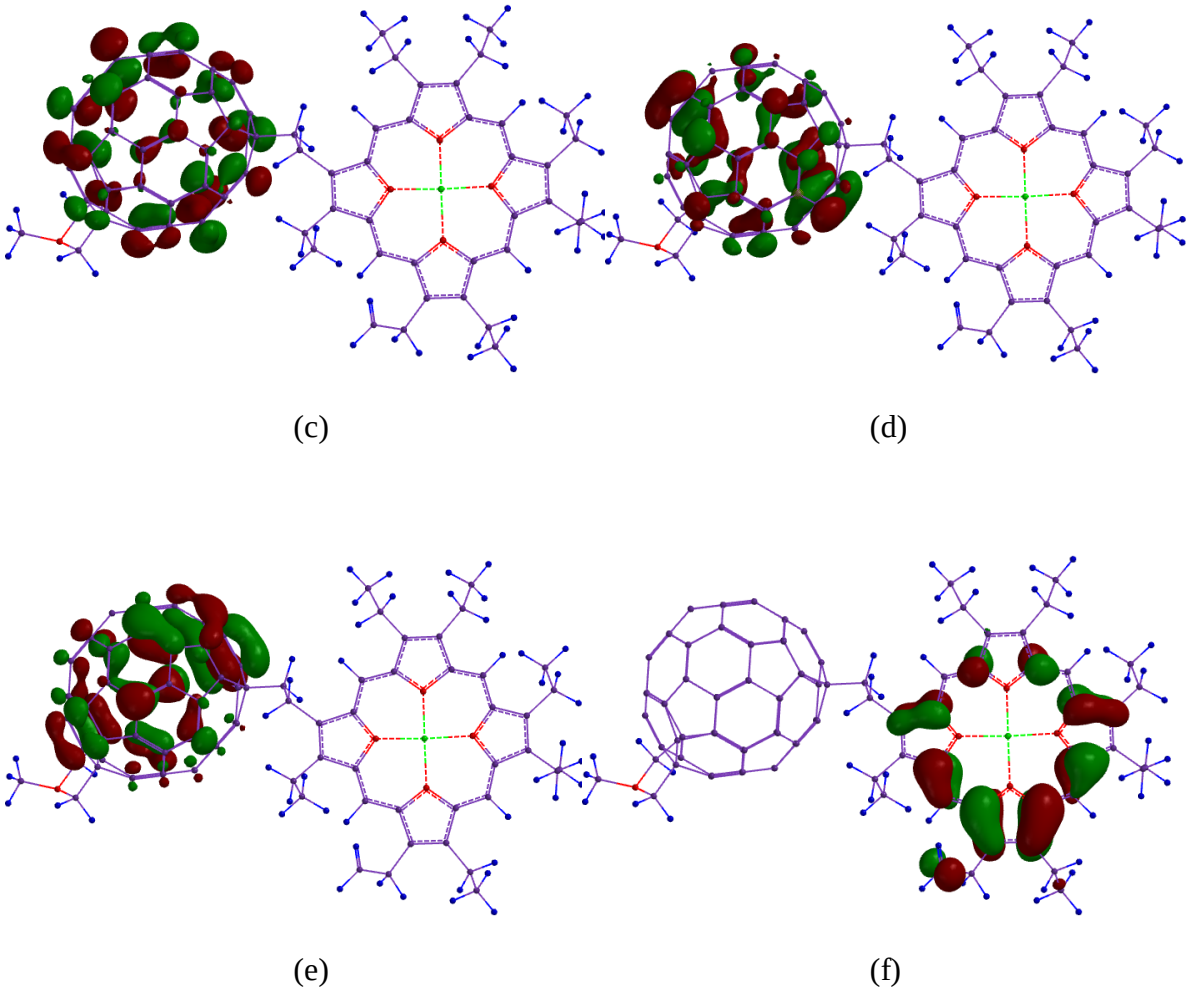

(c) (d)

(e) (f)

Fig. 4. (a) HOMO, (b) HOMO – 1, (c) HOMO – 2, (d) HOMO – 3, (e) HOMO – 4 and (f) HOMO – 5 states of dyad **2** done by HF/3-21G calculations.

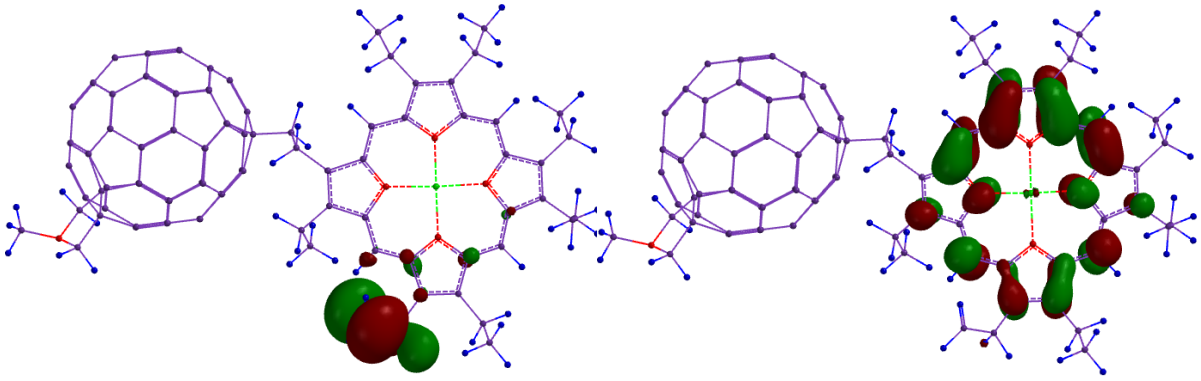

(a) (b)

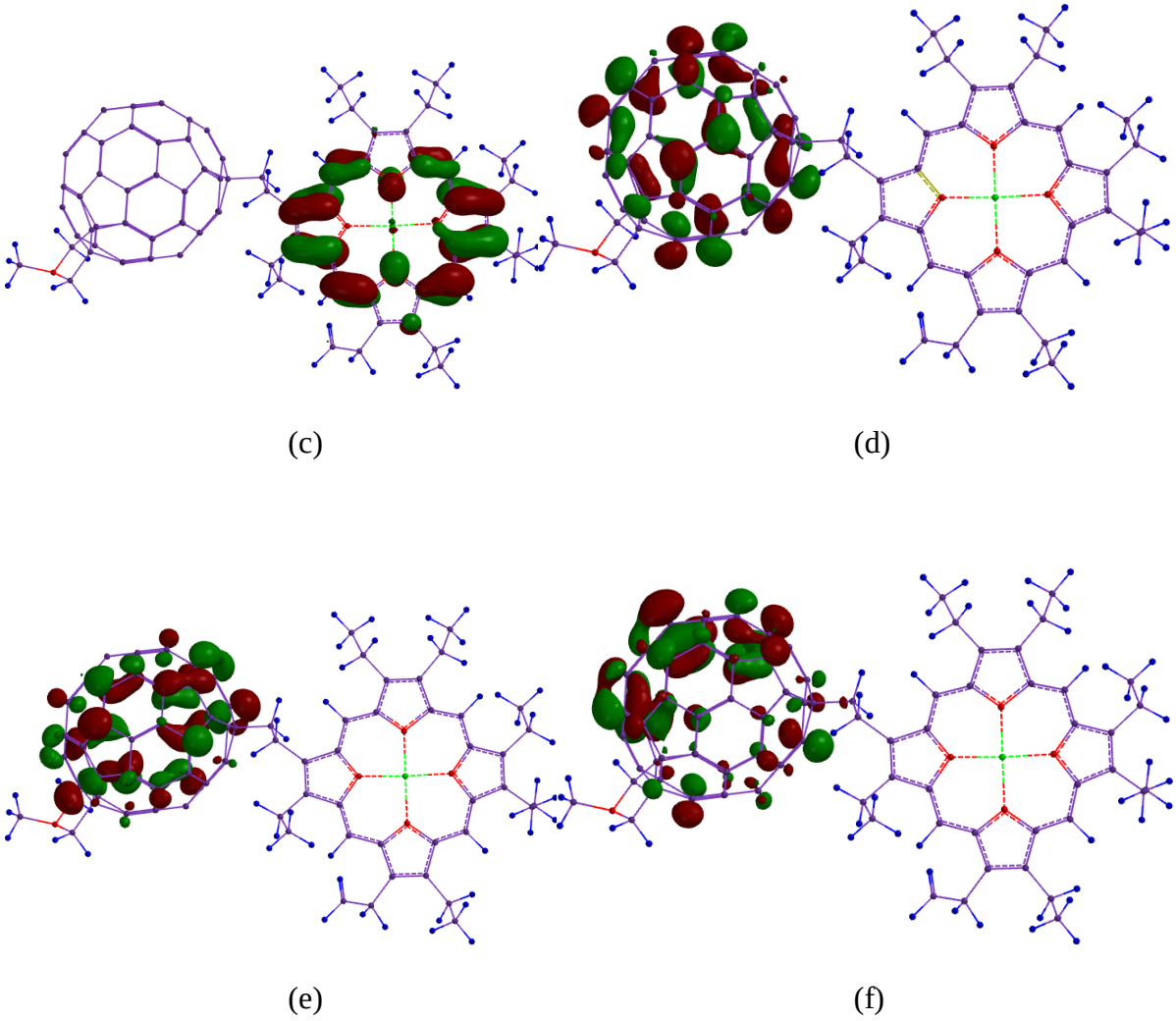

(c) (d)

(e) (f)

Fig. 5. (a) LUMO, (b) LUMO + 1, (c) LUMO + 2, (d) LUMO + 3, (e) LUMO + 4 and (f) LUMO + 5 states of dyad **2** done by HF/3-21G calculations.

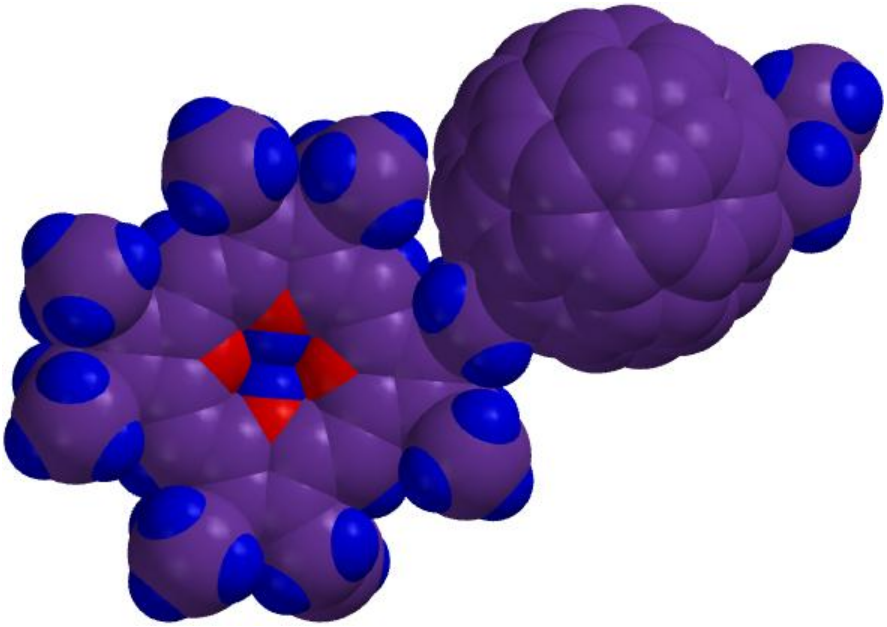

Fig. 6. Space filling model of **1** done by DFT/B3LYP/6-31G* calculations.

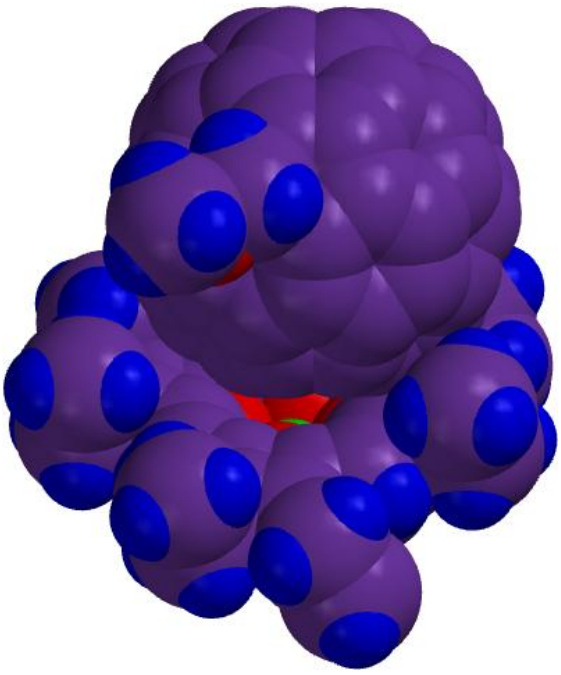

Fig. 7. Space filling model of **2** done by DFT/B3LYP/6-31G* calculations.

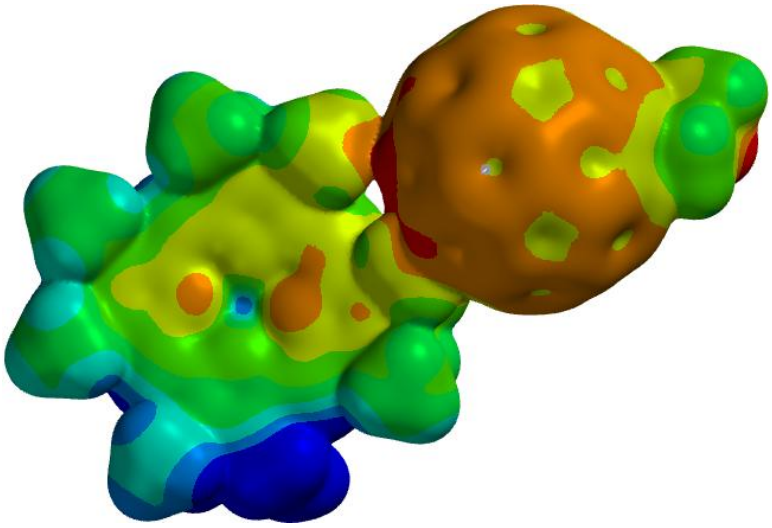

Fig. 8. MEP of dyad **1** done by HF/6-31G* calculations

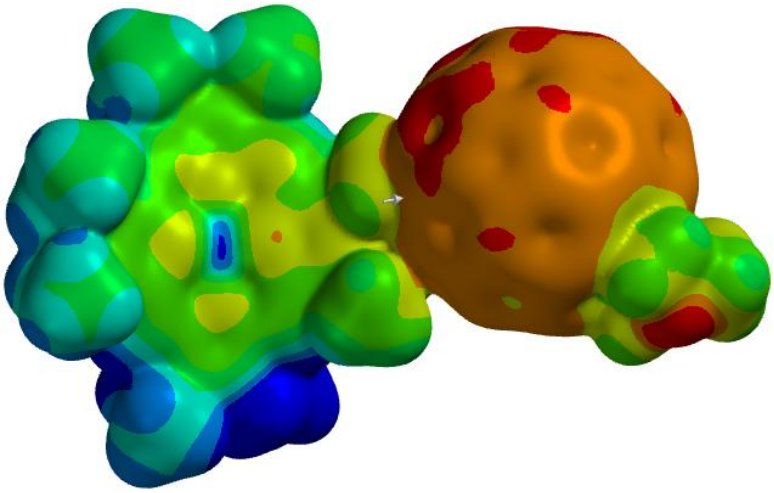

Fig. 9. MEP of dyad **2** done by HF/6-31G* calculations